THE JOURNAL OF PHYSICAL CHEMISTRY B
A JOURNAL OF THE AMERICAN CHEMICAL SOCIETY

pubs.acs.org/JPCB

Perspective

Barrier Crossing Dynamics from Single-Molecule Measurements

Dmitrii E. Makarov*

Cite This: J. Phys. Chem. B 2021, 125, 2467–2476

Read Online

ACCESS | Metrics & More | Article Recommendations

ABSTRACT: Chemists visualize chemical reactions as motion along one-dimensional "reaction coordinates" over free energy barriers. Various rate theories, such as transition state theory and the Kramers theory of diffusive barrier crossing, differ in their assumptions regarding the mathematical specifics of this motion. Direct experimental observation of the motion along reaction coordinates requires single-molecule experiments performed with unprecedented time resolution. Toward this goal, recent single-molecule studies achieved time resolution sufficient to catch biomolecules in the act of crossing free energy barriers as they fold, bind to their targets, or undergo other large structural changes, offering a window into the elusive reaction "mechanisms". This Perspective describes what we can learn (and what we have already learned) about barrier crossing dynamics through synergy of single-molecule experiments, theory, and molecular simulations. In particular, I will discuss how emerging experimental data can be used to answer several questions of principle. For example, is motion along the reaction coordinate diffusive, is there conformational memory, and is reduction to just one degree of freedom to represent the reaction mechanism justified? It turns out that these questions can be formulated as experimentally testable mathematical inequalities, and their application to experimental and simulated data has already led to a number of insights. I will also discuss open issues and current challenges in this fast evolving field of research.

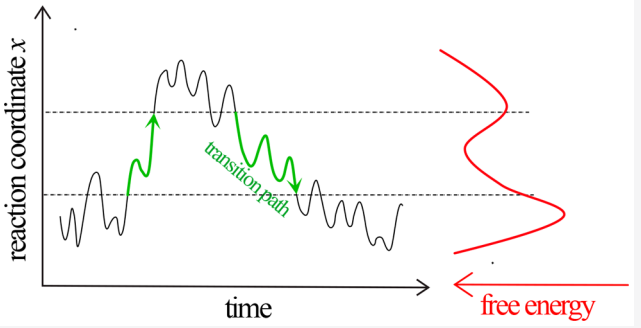

INTRODUCTION

The Arrhenius law expresses the rate k of a chemical reaction in terms of two parameters, the activation (free) energy ΔU and a prefactor ν:

$$k = \nu e^{-\Delta U/k_B T} \quad (1)$$

Here k_B is Boltzmann's constant and T is the temperature. The Arrhenius law is the centerpiece of chemical kinetics, but it has also been applied to phenomena outside traditional physical chemistry such as sliding friction or even collapse of engineering structures.

For complex chemical reactions in condensed phases, first-principles prediction of ΔU and ν is often prohibitive computationally, and even extracting these two parameters from experimentally measured reaction rates k is difficult. Theories of chemical dynamics that aim at predicting the values of ΔU and ν and/or at interpreting experimental data in terms of eq 1 usually invoke the view of a conformational transition as motion along a one-dimensional "reaction coordinate" x (Figure 1) proceeding via a (free) energy bottleneck identified with the "transition state" (TS). Differences among various reaction rate theories developed throughout the 20th century usually lie in the assumptions about this motion and in the definition of the transition state.

In particular, transition state theory usually assumes conservative dynamics, and the TS is viewed as the "point of no return": the system moving along x in the direction toward the reaction product and reaching the TS is committed to reaching the product state. In contrast, Kramers in his famous paper[1] proposed to treat the dynamics along x as Brownian motion in an effective potential $U(x)$. This model offers an attractive description of chemical reactions in solution, where interaction of the molecule of interest with the solvent molecules can be viewed as giving rise to friction as well as to random noise produced by their thermal motion. Within this picture, the transition state is no longer the point of no return; rather, it is a point of "maximum indecision", from which thermal fluctuations can take the system to the product or the reactant with equal probabilities.

Kramers pointed out the limitations of the Brownian motion assumption and the phenomenological character of his model.[1] Brownian motion is a Markov (i.e., memoryless) process, while,

Received: December 8, 2020
Revised: January 27, 2021
Published: February 22, 2021

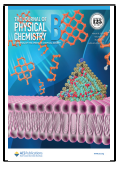

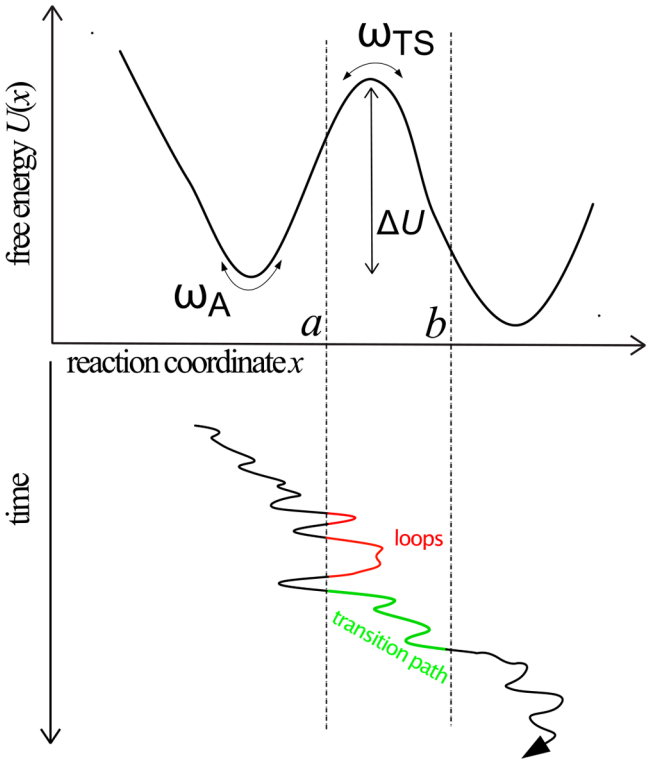

Figure 1. Top: Molecular rearrangements are often viewed conceptually as events where rare thermal fluctuations allow a free energy barrier ΔU to be crossed. Here the potential of mean force $U(x)$ experienced by the molecule along the reaction coordinate x is given by eq 5. The rate of transition is given by the Arrhenius law, eq 1, where the value of the preexponential factor ν strongly depends on the details of the dynamics along x. For example, transition state theory estimates it as $\nu = \omega_A/(2\pi)$, where $\omega_A = \sqrt{U''(\min x)/m}$ is the oscillation frequency in the reactant well (where m is an effective mass), while Kramers' model, in the overdamped limit of the Langevin equation (eq 4), gives $\nu = \frac{m\omega_A\omega_{TS}}{2\pi\gamma} = \frac{\sqrt{U''(\min x)\,|U''(\max x)|}}{2\pi\gamma}$, where γ is the friction coefficient and ω_{TS} is the upside down barrier frequency. Note that the latter result is independent of the mass, as it should be in the overdamped case. Bottom: A transition path (green) is defined as a piece of a molecular trajectory that enters the transition region (a, b) through one of its boundaries (here the boundary a), exits through its other boundary (here the boundary b), and stays continuously within this region in between these two events. Unproductive excursions into the transition region, called loops, enter and exit the transition region through the same boundary (red).

in general, projection of multidimensional dynamics onto a single reaction coordinate leads to non-Markov behavior.[2] In the 1980's, the community of chemical physicists interested in reaction dynamics in solution has extensively explored a particular non-Markovian generalization of the Kramers model, in which the dynamics along x obeys the *generalized Langevin equation* (GLE)

$$m\ddot{x} = -U'(x) - \int_{-\infty}^{t} dt'\xi(t - t')\dot{x}(t') + \zeta(t) \tag{2}$$

GLE is a statement of Newton's second law, with the force (the rhs of eq 2) that includes three terms: a deterministic force whose effect is captured by the potential of mean force $U(x)$, a friction force that depends not only on the instantaneous velocity $\dot{x}(t)$ but also on the velocities in the past, and a Gaussian random noise term $\zeta(t)$. The properties of the last two terms are governed by the friction memory kernel $\xi(t)$, with the autocorrelation function of the noise satisfying the fluctuation−dissipation theorem, $\langle\zeta(t)\zeta(t')\rangle = k_B T\xi(t - t')$. The ordinary Langevin equation, which is the basis of Kramers' theory, is obtained when one eliminates the memory by setting the memory kernel to be proportional to the delta function

$$\xi(t) = 2\gamma\delta(t) \equiv 2\frac{k_B T}{D}\delta(t) \tag{3}$$

where γ is a friction coefficient and D the corresponding diffusivity. This gives

$$m\ddot{x} = -U'(x) - \gamma\dot{x} + \zeta(t) \tag{4}$$

where the noise $\zeta(t)$ is now delta-correlated, $\langle\zeta(t)\zeta(t')\rangle = 2k_B T\gamma\delta(t - t')$. An overdamped limit is usually further assumed for the reaction dynamics in solution. In this limit, the lhs of eq 4 is replaced by zero.

Although the validity of the above models can be and has been tested in application to molecular simulations, experimental observations of biomolecular reactions, until recently, have been limited to measuring reaction rates (eq 1). Capturing further details of molecular motion along a reaction coordinate requires observation of individual trajectories $x(t)$, which necessitates single-molecule techniques. However, the temporal resolution of typical single-molecule experiments is often quite low and insufficient for resolving the dynamic details of molecular transitions. The pioneering studies by the Eaton[3,4] and Woodside[5,6] groups, however, pushed the temporal resolution of, respectively, single-molecule fluorescence resonance energy transfer (smFRET) and single-molecule force spectroscopy (smFS) studies to a microsecond range and permitted observation of *transition paths* (Figure 1), i.e., brief excursions where a large thermal fluctuation allows the system to cross the activation barrier. Despite these achievements, it is worth noting that the impressive temporal resolution achieved experimentally ($\sim$1 μs) is comparable to the temporal length of an entire state-of-the-art atomistic simulation of a typical-size protein in explicit solution! One thus cannot analyze experimental trajectories in the same way as one could study, say, the trajectories generated by integrating eq 4. The purpose of this Perspective is to discuss the emerging approaches to bridging the time scale gap between experimental temporal resolution and that of relevant microscopic time scales and to highlight recent ideas about how we can learn about microscopic details of barrier crossing dynamics from experimental signals.

The specific problem that we wish to address can be stated as follows. Suppose we have an experimental signal $x(t)$ reporting on the motion along a reaction coordinate x. Note that the choice of x is dictated by experimental considerations and is not necessarily "optimal" from a theoretical perspective;[7] thus, x should be viewed as merely some collective variable that reports on the progress of the molecular system of interest from the reactant to the product. Owing to experimental constraints, the time resolution of the signal is low, typically many orders of magnitude lower than that required to resolve, e.g., the thermal velocity along x.[8] Thus, the observed signal $x(t)$ is a significantly smoothed representation of the true dynamics, and this should be taken into consideration by realistic analysis of the data. We then ask: (1) what is the best one-dimensional model that can account for the observed dynamics along x, and (2) what can we say about the underlying microscopic mechanisms of the observed chemical reaction?

https://dx.doi.org/10.1021/acs.jpcb.0c10978
J. Phys. Chem. B 2021, 125, 2467−2476

THE EFFECTIVE POTENTIAL FROM SINGLE-MOLECULE TRAJECTORIES

The most basic characteristic shared by various dynamical models is the potential $U(x)$ appearing in eqs 2 and 4. For a system in equilibrium, this potential can be estimated from a long, ergodic trajectory $x(t)$: by demanding that the equilibrium probability distribution $p_{eq}(x)$ of the coordinate x must be the Boltzmann distribution associated with this potential, one obtains, to within an additive constant,

$$U(x) = -k_B T \ln p_{eq}(x) \tag{5}$$

A practical complication that arises in using eq 5 is that the experimental observable (e.g., the displacement of a dielectric bead in the optical trap) is not identical to the molecular coordinate of interest (e.g., the molecular extension). This issue, which has been the focus of a number of studies (e.g., refs 9 and 10), will not be addressed here in any detail, although below we will discuss dynamic consequences of the coupling between experimental observables and intrinsic molecular reaction coordinates.

A more fundamental limitation of using eq 5 is that it assumes thermal equilibrium and is thus inapplicable to out-of-equilibrium systems. For example, the position x of a molecular motor walking along its track shows the trend to increase or decrease,[11] and thus, an equilibrium distribution $p_{eq}(x)$ does not exist, although a steady-state probability density $p_{ss}(x)$ may be defined for a periodic system by mapping the unbonded trajectory $x(t)$ onto a finite interval equal to the period. Diffusion in the tilted periodic potential is a simple model illustrating this kind of dynamics (Figure 2).

Three types of solutions to the problem of determining the effective potential in nonequilibrium systems have been proposed recently. All three are based on the same model of the Langevin equation without memory (eq 4) in the overdamped limit, where the acceleration term in the lhs of eq 4 can be neglected.

The first approach[12−15] takes advantage of the equivalent Smoluchowski description of the system (see, e.g., refs 2 and 16) and assumes that steady state exists in the system. The Smoluchowski equation, then, provides an expression for the steady-state flux j_{ss}

$$j_{ss} = -\gamma^{-1}U'(x)p_{ss}(x) - \gamma^{-1}k_B T p'_{ss}(x) \tag{6}$$

from which one readily finds

$$-\gamma^{-1}U'(x) = j_{ss}/p_{ss}(x) + \gamma^{-1}k_B T \, \mathrm{d}\ln p_{ss}(x)/\mathrm{d}x \tag{7}$$

and the potential $U(x)$ can be obtained by integrating the above equation. In equilibrium, $j_{ss} = 0$, $p_{ss}(x) = p_{eq}(x)$, and one recovers eq 5. A drawback of this approach is that it requires an advance knowledge of the friction coefficient γ, although in certain nonequilibrium scenarios this is not necessary.[13]

The second approach is based on the *splitting probabilities* defined in the following way. Let x be some point within the interval (a, b), which can be chosen arbitrarily but is usually taken to be in the barrier region (Figure 1). The splitting probability $\phi_a(x)$ is the probability that a trajectory starting from x will cross the interval boundary a before crossing the boundary b, and $\phi_b(x) = 1 - \phi_a(x)$ is the probability that the boundary b will be crossed before a. The quantity $\phi_b(x)$ is also known as the "committor" or "pfold".[7] Under the assumption of overdamped Langevin dynamics (eq 4), the underlying potential $U(x)$ can be estimated, to within an additive constant, from the splitting probabilities as

$$U(x) = k_B T \ln \frac{\mathrm{d}\phi_b(x)}{\mathrm{d}x} \tag{8}$$

Notably, the value of the friction coefficient does not enter into eq 8. Equation 8 is true regardless of whether or not the system is in equilibrium, and it has already been used to reconstruct potentials of mean force from single-molecule force spectroscopy data in the equilibrium case.[17,18] Its utility for nonequilibrium systems was demonstrated using synthetic data in our recent paper.[19]

The third approach[20,21] is based on the proportionality of the local drift velocity to the local force (i.e., the gradient of the potential). An advantage of this approach is that, in principle, it allows for a more general dynamical model where the diffusivity is coordinate-dependent (and offers a method for measuring this dependence). A disadvantage is that it requires high temporal resolution/data sampling rate, so it is more suitable for analyzing processes with slow dynamics.

IS DYNAMICS MARKOVIAN?

The theory of Brownian motion was developed to describe the motion of micron-sized particles in solution. Applicability of Stokes' law, which predicts a friction force that is proportional to the particle's velocity and gives the value of the friction coefficient γ as a function of the particle's size and the solvent viscosity, justifies the use of the Langevin equation. In contrast, there is little physical basis for using eq 4 as a description of motion along a molecular degree of freedom x, and the microscopic origin of the friction coefficient γ is not fully understood.[22] General theoretical considerations[2] indicate that, when a low-dimensional projection (i.e., coordinate x) of a multidimensional dynamics (i.e., the motion of the molecule and the surrounding solvent) is considered, its time evolution is generally non-Markovian (i.e., it displays memory effects). Quoting van Kampen,[23] "Non-Markov is the rule, Markov is the exception".

Even if the intrinsic dynamics along the molecular coordinate x is Markovian, experiments rarely observe it directly. Instead, one usually monitors another degree of freedom y associated with the experimental setup, such as the displacement of a dielectric bead attached to the molecule via a polymeric handle (Figure 3). The coupling between these two degrees of freedom causes the dynamics of both x and y to be non-Markovian even if their dynamics are Markovian when they are decoupled.[24] More precisely, even if the dynamics of the combined system described by the pair of variables (x, y) is Markovian, the dynamics of x or y alone is not. In particular, in the simple model where the coupling between x and y is represented as a Hookean spring,[9,25−27] it introduces an exponentially decaying term in the friction kernel $\xi(t)$ describing the dynamics (eq 2) of x.[16,28]

Given an observed trajectory $x(t)$ (or $y(t)$), can one tell whether or not it obeys a Markovian process? Recently, we have found two rigorous inequalities that enable one to do so. The first one[29] is concerned with the probability $p(x|a \to b)$ that a point x that is located within the transition region, $a < x < b$, belongs to a transition path from a to b rather than to a "loop" that enters and exits the transition region through the same boundary (see Figure 1). For a Markov process that satisfies time-reversal symmetry, one can divide any $a \to b$ transition path into the $a \to x$ and $x \to b$ segments and use their statistical

https://dx.doi.org/10.1021/acs.jpcb.0c10978
J. Phys. Chem. B 2021, 125, 2467−2476

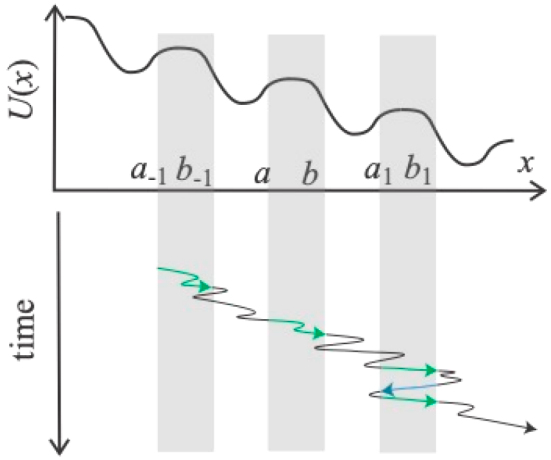

Figure 2. A simple model of a periodic nonequilibrium system. Tilted periodic potential $U(x)$ results in overall drift of the system from left to right. Models of this type have been used as minimal descriptions of molecular motors walking along periodic tracks. By mapping transition paths traversing periodically repeated intervals (a_n, b_n) onto a single interval (a, b), one can study statistical properties of the transition path ensemble. Note that, in general, forward (from a to b) and backward (from b to a) transition paths are observed even if the latter may be rare.

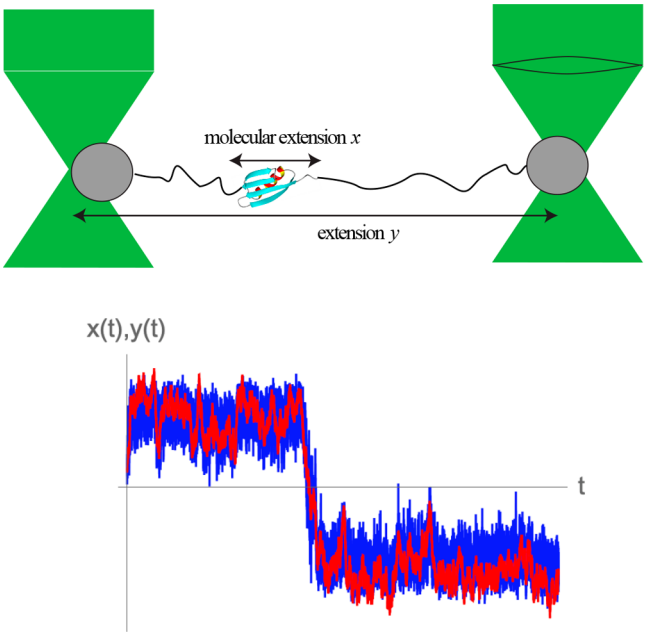

Figure 3. Top: In an optical tweezers setup, the molecular extension x is reported by another coordinate y, which is related to the locations of beads in optical traps. Bottom: A molecular transition as manifested in the dynamics of a molecular coordinate $x(t)$ (blue) and as observed experimentally (here, in a simulated experiment) in the dynamics of $y(t)$ (red).

independence, along with the time reversibility of the $a \to x$ trajectory segment, to show that $p(x|a \to b) = \phi_a(x)\phi_b(x) = [1 - \phi_b(x)]\phi_b(x)$. As the splitting probability $\phi_b(x)$ varies between 0 and 1, $p(x|a \to b)$ attains its maximum value of 1/4 at the "transition state" defined by $\phi_b(x) = 1/2$. For non-Markov overdamped dynamics, however, it can be shown[29] that the following inequality holds

$$p(x|a \to b) \leq 1/4 \tag{9}$$

for any $x \in (a, b)$. If the maximum of the function $p(x|a \to b)$ is found to be below 1/4, then, the observed process must be non-Markov. Indeed, such deviations from Markovianity have been observed both in experiments[24,30] and in simulations of protein dynamics,[29,31] although the physical origins of memory are not necessarily the same in these cases, since the coupling to the experimental probe may be the main source of non-Markov effects in the experimental studies.

The second inequality is concerned with the distribution of the transition path time, $p_{TP}(t)$, i.e., the temporal length of a transition path. Specifically, the width of the distribution can be quantified by its coefficient of variation

$$C = \frac{(\langle t_{TP}{}^2\rangle - \langle t_{TP}\rangle^2)^{1/2}}{\langle t_{TP}\rangle} \tag{10}$$

where $\langle t_{TP}\rangle = \int_0^\infty t p_{TP}(t)\, dt$ is the mean transition path time and $\langle t_{TP}{}^2\rangle = \int_0^\infty t^2 p_{TP}(t)\, dt$ is the second moment of the distribution. A small value of C indicates a narrow distribution that is sharply peaked around its mean. A large value of C, on the other hand, indicates a broad distribution. A single-exponential distribution provides a demarcation line between these two cases, with $C = 1$. We proved[32] that, for any one-dimensional diffusion model (i.e., one based on eq 4 in the overdamped limit), the coefficient of variation is always lower than 1. Thus, if a value $C > 1$ is measured, this unambiguously invalidates a one-dimensional description based on eq 4 and necessitates use of a non-Markovian model to describe the data. For a symmetric parabolic barrier, one can further show[32] that the value of C cannot exceed $\sqrt{2/5} \approx 0.63$, which is the value calculated for a constant potential $U(x)$. This suggests an even more stringent Markovianity criterion, $C < 0.63$, for systems whose potential of mean force exhibits a barrier (or, at least, one with a shape close to parabolic), although it is unclear whether this result can be generalized to barriers of arbitrary shapes.

IF DYNAMICS IS NON-MARKOVIAN, THEN WHAT KIND OF DYNAMICS IS IT AND WHAT IS ITS PHYSICAL ORIGIN?

For most chemists and physicists, Markovian stochastic dynamics is synonymous with diffusion (i.e., overdamped Langevin dynamics) in the continuous case and with master-equation dynamics in the discrete case.[2] Non-Markovian models, in contrast, may display anomalous diffusion and come in all shapes and sizes.[33] Thus, a mere finding that the motion along x exhibits memory and/or anomalous diffusion does not tell us enough about its physical nature, as will be illustrated below.

The GLE, eq 2, is, perhaps, the most common non-Markov model in chemical reaction dynamics. If the GLE is an adequate description, then the friction memory kernel $\xi(t)$ can be deduced directly from an ergodic trajectory $x(t)$.[34−37] In particular, in the case of overdamped dynamics, its Laplace transform, $\hat{\xi}(s) = \int_0^\infty e^{-st}\xi(t)$, is given by[36]

$$\hat{\xi}(s) = \frac{\hat{C}_{fx}(s)}{s\hat{C}_{xx}(s) - \hat{C}_{xx}(0)} \tag{11}$$

where $\hat{C}_{xx}(s)$ and $\hat{C}_{fx}(s)$ are the Laplace transforms of the position autocorrelation function, $C_{xx}(t) = \langle x(0)x(t)\rangle$, and of the force−position correlation function, $C_{fx}(t) = -\langle x(0)$

https://dx.doi.org/10.1021/acs.jpcb.0c10978
J. Phys. Chem. B 2021, 125, 2467−2476

$U'[x(t)]\rangle$. Importantly, the time resolution of the above correlation functions does not need to match the characteristic time scale of the memory kernel. In particular, even in the extreme of infinitely short memory (i.e., the Markov limit, eq 3), eq 11 can still be used to determine the friction coefficient γ. Indeed, utility of eq 11 has been tested in application to experimentally observed dynamics of a micrometer-sized dielectric bead in a dual optical trap[38] and in application to simulated loop closure dynamics in intrinsically disordered proteins.[39]

As noted above, one of the rigorously justifiable applications of the GLE is to describe the dynamics of a molecular reaction coordinate x coupled to an experimental observable y (Figure 3). Interestingly, the criterion based on eq 9 detects such experimental-probe-induced non-Markovianity,[24,30] yet extensive simulations suggest that the coefficient of variation, eq 10, remains less than 1 in this case[32] provided that the dynamics along x in the absence of coupling to y is Markovian. At this point, we do not have a proof of this observation, nor do we know whether a GLE with an arbitrary friction memory kernel (rather than an exponential kernel obtained in the case of bilinear coupling between x and y) can result in a transition path time distribution with $C > 1$. Nevertheless, the observation that coupling to the experimental probe can result in non-Markovian dynamics that is detectable via application of eq 9 but not necessarily resulting in a coefficient variation C being greater than 1 has important experimental implications. Specifically, different physical mechanisms of memory may produce different experimental signatures. As a consequence, proper analysis of experimental data can help one narrow down the physical origin of the memory effects. In particular, we know that values of $C > 1$ are observed in atomistic simulations of protein dynamics[32] (although experimental evidence is lacking at this point), and we (tentatively) know that coupling to the experimental probe *per se* does not lead to values of $C > 1$. Thus, if a broad distribution of transition path times with $C > 1$ is found experimentally, it would be likely to originate from intrinsic non-Markovianity of the motion along the molecular reaction coordinate rather than from the molecule's coupling to the experimental probe.

The observation that GLE dynamics does not (necessarily) lead to broad distributions of transition path times raises the question: what kind of dynamics does? Certain models that display anomalous diffusion[40] do lead to values of C exceeding 1, but how do we select the right model from a vast menu of existing non-Markov models?[33] It is helpful to restate this question differently. Memory is generally a result of the coupling of the degree of freedom of interest x to other, unobserved degrees of freedom. Let us denote those y and, for the sake of (extreme) simplicity, assume that there is only one such degree of freedom. The dynamics in the (x, y) space is Markovian, but when we observe x alone, we find that a non-Markovian description has to be invoked. Let $V(x, y)$ be the underlying (free) energy landscape describing this 2D system. We then ask, what properties must $V(x, y)$ have in order to lead to the observation of a broad distribution of transition path time measured using x alone as a reaction coordinate?

Energy landscapes of biomolecules are generally rough, exhibiting many local minima. This roughness may lead to multiple pathways between the initial and final states. Such pathway heterogeneity may lead to a broad distribution $p_{TP}(t)$, as can be seen from the simple model with just two parallel pathways[32] (Figure 4A). Suppose $p_{TP}^{(1)}(t)$ and $p_{TP}^{(2)}(t)$ are the distributions of the transition path time corresponding to the

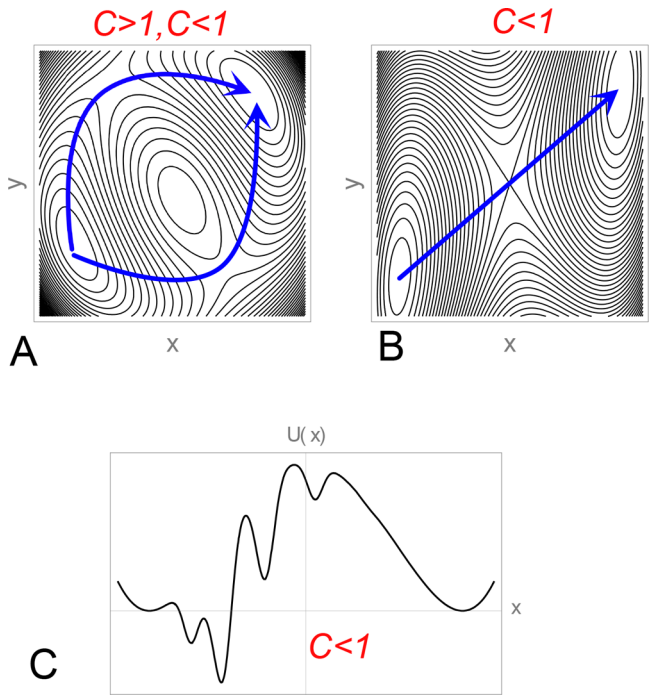

Figure 4. (A) Bumpy free energy landscapes with multiple saddle points and thus multiple reaction pathways may lead to a broad distribution of the transition path time when the dynamics is projected onto a single reaction coordinate x. Here this is illustrated for a two-pathway landscape with two saddles, where the distribution's coefficient of variation C may or may not exceed 1 depending on the landscape's details (see eq 13). (B) In contrast, simple harmonic coupling of the reaction coordinate x to another degree of freedom y (shown is a contour plot of the free energy landscape described by eq 14) does not (necessarily) lead to a broad distribution of the transition path time measured along x, as reflected by values of the coefficient of variation C below unity found in simulation studies.[32] (C) Importantly, roughness of the free energy landscape alone does not necessarily lead to a broad distribution $p_{TP}(t)$: The coefficient of variation C is always less than 1 for diffusive dynamics in any one-dimensional potential, no matter how rugged it is. For a recent discussion of the effect of energetic roughness of the transition path times in 1D potentials, see refs 41 and 42.

first and second pathways and f_1 and $f_2 = 1 - f_1$ are the fractions of transition paths proceeding via each pathway. Then, the overall distribution of the transition path time is given by

$$p_{TP}(t) = f_1 p_{TP}^{(1)}(t) + f_2 p_{TP}^{(2)}(t) \tag{12}$$

Even if the distributions $p_{TP}^{(1)}(t)$ and $p_{TP}^{(2)}(t)$ are narrow, with individual coefficients of variation $C_1 < 1$, $C_2 < 1$, the distribution given by eq 12 may be broad, with its coefficient of variation obtained from eqs 10 and 12

$$C = \left[\frac{f_1 \langle t_1^2 \rangle + f_2 \langle t_2^2 \rangle}{(f_1 \langle t_1 \rangle + f_2 \langle t_2 \rangle)^2} - 1 \right]^{1/2} \tag{13}$$

exceeding 1. More precisely it can be shown[32] that C always exceeds 1 provided that the ratio of the mean transition path times $\langle t_{TP}^{(2)} \rangle / \langle t_{TP}^{(1)} \rangle$ corresponding to each pathway is sufficiently large or small. In other words, disparity in the mean transition path times corresponding to different pathways is the origin of a broad distribution with $C > 1$.

In contrast, a single-pathway model (Figure 4B) with the free energy landscape given by

https://dx.doi.org/10.1021/acs.jpcb.0c10978
J. Phys. Chem. B 2021, 125, 2467−2476

$$V(x, y) = U(x) + k(y - x)^2/2 \quad (14)$$

where $U(x)$ is the potential of mean force for the reaction coordinate x, was found[32] to give $C < 1$. Given that the free energy landscape of eq 14 is commonly used to describe the coupling of the molecular reaction coordinate x to the degrees of freedom y of the experimental probe,[9,18] such coupling then is unlikely to result in a broad distribution of the transition path time with $C > 1$, as already noted above.

To further complicate matters, it is not true that any single-pathway model would lead to a value of C less than 1. A free energy surface with a single saddle but with a "broad" saddle region was also shown to exhibit an ensemble of transition path times that is heterogeneous enough to lead to a value of C exceeding 1.[32] The key property of the underlying free energy landscape that leads to broad ($C > 1$) distributions, then, is not the energetic roughness but the existence of parallel pathways, a situation that is impossible in one dimension. Note that roughness of a one-dimensional free energy landscape also leads to broadening of the distribution $p_{TP}(t)$, as recently shown experimentally[41] for a *de novo* designed protein. However, no matter how rough (Figure 4C), a one-dimensional free energy landscape cannot lead to a distribution $p_{TP}(t)$ that is broader than single-exponential ($C > 1$), assuming diffusive (i.e., Markovian) dynamics on this landscape.

The same conclusion can be reformulated in a discrete language: If the system of interest is modeled as a network of discrete states whose populations obey a master equation (i.e., is, in modern parlance, a Markov-state model), then the transition path time distribution is always narrower than a single-exponential one ($C < 1$) if the network is linear, but it can be broader than a single exponential one ($C > 1$) for a network of nonlinear topology. In a chemist's language, such nonlinear networks feature off-pathway intermediates leading to heterogeneous ensembles of transition paths.

Heterogeneity of transition path ensembles has recently been suggested by experimental studies[43,44] and is also evident in simulations.[32,45] Unfortunately, this is a property that is somewhat fuzzy and hard to quantify. The coefficient of variation of the distribution $p_{TP}(t)$ appears to provide a useful proxy for the ensemble heterogeneity, but whether better, more direct measures of this property exist remains an open question.

QUANTIFYING TRANSITION PATH SHAPES

The transition path time is the property of the transition path ensemble that is most readily accessible experimentally. However, as the spatial and temporal resolution of experimental studies is being improved, other properties become accessible as well. Perhaps the most obvious question that one can ask about transition paths is what they "look like". That is, what are their typical, or average, shapes?

The question of the average path shape is nontrivial. Consider the set of transition paths $x(t)$ shown in Figure 5. Since each spans a time interval of different length, it makes no sense to calculate the average value of the coordinate x measured at a given time t. To overcome this difficulty, one can restrict the average to the paths of fixed temporal length t_{TP} (which can further be chosen to be equal to the mean transition path time $\langle t_{TP} \rangle$), resulting in the average transition path $\langle x(t|t_{TP}) \rangle$ conditional upon a fixed transition path time.[44] Instead, one can view the path as a function $t(x)$,[46] with x now being confined to the transition region, $a < x < b$. Unlike $x(t)$, however, the function $t(x)$ is not single-valued, since a transition path can cross the same point x times. This problem is solved by considering only the average first (last) crossing time,[46] $\langle t_{\text{first(last)}}(x) \rangle$, its symmetrized (and thus time-reversible) version[47] $\frac{\langle t_{\text{first}}(x) \rangle}{2} + \frac{\langle t_{\text{last}}(x) \rangle}{2}$, or an average over all of the crossings.[48] Experimental measurements of these average transition path shapes have been recently reported.[38,44]

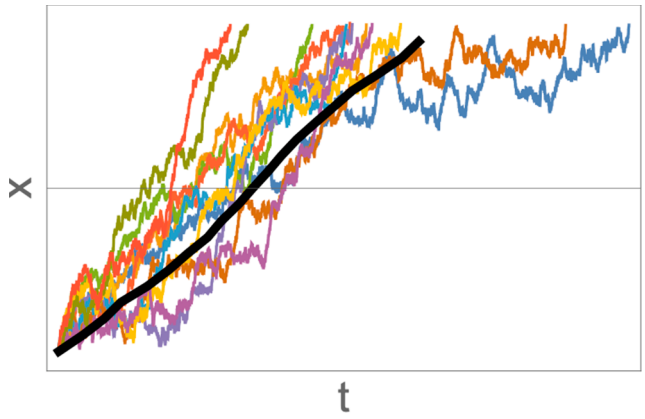

Figure 5. The average transition-path shape. The ensemble of transition paths contains trajectories with varied temporal length, and thus, defining the average shape by computing the average, over all transition paths, value of $x = x(t)$ at a given time t is meaningless, unless only the subensemble of transition paths of fixed temporal duration is considered. Alternatively, the average shape can be defined by computing the average time $t(x)$ at which a transition path crosses the point x for the first or last time, or the mean of the first and last crossing times. The latter choice of the average shape is shown as the thick black curve.

Another (in the author's view more appealing) way of characterizing average properties of transition paths is based on the "transition path" velocity[8,49] $v_{TP}(x)$. This quantity is, in general, quite different from the instantaneous thermal velocity with which a point x is crossed. In fact, the typical thermal velocity is many orders of magnitude too fast to be measurable given the current time resolution of single-molecule measurements. In contrast, $v_{TP}(x)$ is a coarse-grained velocity and is typically much lower than the thermal velocity. It is defined as

$$\frac{1}{v_{TP}(x)} = \langle t_{TP} \rangle p(x|TP) \quad (15)$$

where $p(x|TP)$ is the probability density of all points x belonging to transition paths. Equation 15 reflects the intuitive notion that a faster moving particle spends less time around a point x and so the probability of finding it near point x should be inversely proportional to velocity.

Transition path velocity is a "nearly equilibrium" property in that it only requires the (conditional) distribution $p(x|TP)$ of transition path points. As such, it is measurable with relatively modest time resolution comparable to that required to resolve transition path times. It further satisfies several mathematical identities that make it appealing. First, in support of this quantity as a "velocity", one can prove[8] the following identity:

$$\int_a^b \frac{dx}{v_{TP}(x)} = \langle t_{TP} \rangle \quad (16)$$

Second, there is a useful general identity that relates the (reactive) flux of transition paths $F_{a\to b}$ from the boundary a to the boundary b to the transition path velocity.[8] In the

https://dx.doi.org/10.1021/acs.jpcb.0c10978
J. Phys. Chem. B 2021, 125, 2467−2476

particularly interesting case of diffusive dynamics along x, this identity takes the form

$$F_{a\to b} = \frac{1}{4} v_{\mathrm{TP}}(x^*) p_{\mathrm{eq}}(x^*) \tag{17}$$

where x^* is the transition state point defined by $\phi_a(x^*) = \phi_b(x^*) = 1/2$ and $p_{\mathrm{eq}}(x)$ is the equilibrium probability density. In the case where the transitions between the two basins of attraction separated by the interval (a, b) can be described by first order kinetics, the reactive flux can further be written as $F_{a\to b} = k_{a\to b} P_a$, where $k_{a\to b}$ is the transition rate coefficient and $P_a = \int_{-\infty}^{a} \mathrm{d}x p_{\mathrm{eq}}(x)$ is the equilibrium population of the reactant state (i.e., the left basin)—see Figure 1. Equation 17 is remarkably similar to the transition-state-theory expression for the reactive flux

$$F_{a\to b}^{\mathrm{TST}} = k_{a\to b}^{\mathrm{TST}} P_a = \frac{1}{2} \langle |v| \rangle p_{\mathrm{eq}}(x_{\mathrm{TS}}) \tag{18}$$

where v is the thermal velocity and x_{TS} is the position of the transition state. In fact, both eq 17 and eq 18 can be derived as limiting cases of the more general relation between the transition path velocity and the reactive flux.[8] Crudely speaking, the exact transition rate can be written in the transition-state-theory-like form if the transition path velocity is used instead of the thermal velocity.

Finally, an exact analytical expression for $v_{\mathrm{TP}}(x)$ can be derived in the case of diffusive dynamics.[8] In particular, for the important case of diffusive transitions across a symmetric parabolic barrier, $U(x) = kx^2/2$, $a = -b$, one finds, for the transition path velocity at the barrier top,

$$v_{\mathrm{TP}}(0) = D\sqrt{\frac{8k}{\pi k_{\mathrm{B}} T}}\ \mathrm{erf}^{-1}(\sqrt{\Delta}) \tag{19}$$

where $\Delta = \frac{ka^2}{2k_{\mathrm{B}}T}$ and $D = k_{\mathrm{B}}T/\gamma$ is the diffusivity.

Once the transition path velocity is known, the corresponding transition path shape $x_{\mathrm{TP}}(t)$ can be defined as the inverse of the function $t(x_{\mathrm{TP}})$ given by the integral:

$$\int_a^{x_{\mathrm{TP}}} \frac{\mathrm{d}x}{v_{\mathrm{TP}}(x)} = t(x_{\mathrm{TP}}) \tag{20}$$

If "typical" transition paths are in some sense similar, or, in other words, if the distribution of possible transition paths is sufficiently sharply peaked, then we would expect the various definitions described above to result in similar transition path shapes. Moreover, we would expect all of them to be close to the dominant, or most probable, transition path. Note that, although dominant transition paths are not easily accessible experimentally, they can be described theoretically and they can be computed for systems obeying diffusive dynamics.[50] Indeed, such a similarity among the dominant paths and the various average transition paths was found in simulations and theoretical studies of diffusive crossing of one-dimensional barriers.[8,47] Experimentally, however, significant differences were found between $\langle x(t|t_{\mathrm{TP}}) \rangle$, the average shape in the spatial domain, and $\langle t(x) \rangle$, the average shape in the time domain, for the folding/unfolding transitions of DNA hairpins.[44] This difference may hint at heterogeneity of the transition path ensemble, which was discussed above.

TRANSITION PATHS IN NONEQUILIBRIUM SYSTEMS

Perhaps the most exciting future application of single-molecule measurements of transition paths is to the dynamics of molecular machines. Mechanistic experimental information about, e.g., how molecular motors generate mechanical force is scarce, and direct experimental observation of a motor's trajectory during critical (but short) phases where it undergoes large displacements moving from one metastable state to another could provide a wealth of information.

Molecular machines operate away from equilibrium. Properties of transition path ensembles in such nonequilibrium systems have attracted recent attention.[51−53] One intriguing question is concerned with the forward/backward symmetry of transition paths. In equilibrium, the statistical properties of transition paths that traverse the transition region from a boundary a to a boundary b (see Figure 1; let us call such paths the forward ones) are identical to those of the backward transition paths (going from b to a).[54−56] This is a direct consequence of the time reversal symmetry, as forward transition paths are time-reversed backward transition paths. Such symmetry may however be broken when the system is driven by an external, time-dependent force, as recently shown experimentally.[52]

Breaking of the forward/backward symmetry by nonequilibrium systems without external time-dependent driving is a more subtle question.[53] Consider, for example, the dynamics in a tilted periodic potential shown in Figure 2. Using periodicity of the system, we can map all transition paths traversing periodically replicated transition regions (a_n, b_n) onto a single interval (a, b). Let $p_{a\to b}(t)$ and $p_{b\to a}(t)$ be the distributions of the forward and backward transition path times. Are these distributions the same or different? In the case of diffusive dynamics, the two distributions turn out to be identical despite the lack of equilibrium and despite the overall directional motion of the system.[53] The same conclusion can be drawn about other properties of the forward and backward transition paths. This finding implies, for example, that the "forward stroke" of a molecular motor is, statistically, the time reverse of the backward stroke[57] as long as the 1D diffusion description is applicable.

However, the conclusion changes when the dynamics along x is non-Markovian.[53] In this case, one generally finds that $p_{a\to b}(t) \neq p_{b\to a}(t)$, although the time reversal symmetry necessitates that the two distributions are still identical in equilibrium. In other words, the symmetry between the forward and backward transition paths is broken only when two conditions are met simultaneously: the process is a nonequilibrium one, and the dynamics of the observed reaction coordinate is non-Markovian.[53]

OUTLOOK

In recent years, single-molecule experiments have revealed barrier crossing events in biomolecules with increasing spatial and temporal resolution.[58,59] Studies of transition paths in biomolecular folding have been extended to protein binding[31,43,60,61] and to nonequilibrium systems.[52] At the same time, several theoretical models (such as the Langevin equation and the GLE) have been explored as candidates for low-dimensional descriptions of experimental data. At this point, there appears to be a disconnect between theory/simulations and experiments in that the simple 1D diffusion model often seems to be an adequate description of transition paths observed experimentally,[30,62] yet it commonly[22,40,63] (but not always[64]) fails as a

https://dx.doi.org/10.1021/acs.jpcb.0c10978
J. Phys. Chem. B 2021, 125, 2467−2476

description of transition paths observed in simulations. It is possible that the origin of this discrepancy lies in the difference in the systems studied. For example, experimentalists may favor proteins with slower folding dynamics, which present less stringent demands on the time resolution, while computational biophysicists prefer fast folders (with low folding barriers), as they impose less stringent demands on the simulation length—since the distribution of the transition path time tends to be broader (as quantified by the coefficient of variation C) for low barriers,[32,60] memory effects on this distribution may be easier to detect in such lower-barrier systems, while the value of C may remain below 1 in high-barrier systems even when memory effects are significant.

Experimental artifacts caused by the coupling of the molecular degrees of freedom to the experimental probes present another hurdle to a meaningful comparison between theory/simulations and experiments; although those artifacts have received considerable recent attention, reconstruction of the intrinsic molecular dynamics from experimental observables remains a difficult inverse problem. Notwithstanding these issues, convergence of the experimental and simulational time scales seems within reach at this point.

One interesting theoretical issue suggested by recent simulation studies of transition paths is that of an adequate low-dimensional theoretical description of barrier crossing dynamics in systems with memory. As discussed above, the GLE (eq 2) is one possible description of memory, which has been studied extensively in modern theory of reaction dynamics (see, e.g., ref 16) and which has already been explored as a theoretical description of transition path times.[28,51,65] It appears, however, that the GLE does not capture long tails of the distributions of transition path times observed in atomistic simulations,[39] and it generally predicts distributions that are narrower than the observed ones.[32] If not GLE, what are the alternatives? This question remains open, but given the renewed interest in non-Markov processes reflected in recent publications in mathematics, physics, and chemistry (see, e.g., refs33, 66, and 67), other mathematical models of non-Markov dynamics may soon emerge as better descriptions of experimental observations.

Another open question is how to quantify the heterogeneity of the transition path ensembles suggested by experimental[43,44] and theoretical[32,45,68] studies. For simple systems, heterogeneity is easy to understand intuitively. For example, a reaction that can occur via two parallel pathways (Figure 4A) obviously has a more heterogeneous ensemble of transition paths than a single-pathway reaction (Figure 4B). However, biomolecular dynamics often requires models that involve complex networks of states, and how to quantify which networks lead to more heterogeneous dynamics is not obvious. Given that heterogeneity affects how broad the distribution of the transition path time is,[32] the coefficient of variation of this distribution is a possible heterogeneity measure, but more direct and intuitive measures are desirable.

In conclusion, single-molecule observations of fast barrier crossing dynamics offer a window into the elusive biomolecular reaction mechanisms as well as a critical test of chemical dynamics theories developed in the past. In the near future, we expect broader use of more sophisticated experimental techniques that can monitor several dynamical variables at once,[43] extension of the scope of such studies to include molecular machines, and theoretical efforts to address new fundamental challenges presented by these studies.

AUTHOR INFORMATION

Corresponding Author

Dmitrii E. Makarov − *Department of Chemistry and Institute for Computational Engineering and Sciences, University of Texas at Austin, Austin, Texas 78712, United States;* orcid.org/0000-0002-8421-1846

Complete contact information is available at: https://pubs.acs.org/10.1021/acs.jpcb.0c10978

Notes

The author declares no competing financial interest.

Biography

Dmitrii E. Makarov received a PhD in theoretical physics from the Institute for Chemical Physics (Moscow, Russia) in 1992. Since 2001, he has been on the faculty at the Department of Chemistry at the University of Texas at Austin. He is also a core faculty member at the Oden Institute for Computational Engineering & Sciences. His research interests are in the field of computational and theoretical chemical physics, with current research topics ranging from quantum reaction rate theory to molecular biophysics.

ACKNOWLEDGMENTS

I am grateful to Alexander M. Berezhkovskii and Rohit Satija for numerous discussions of the topics presented here. Financial support by the Robert A. Welch Foundation (Grant No. F-1514) and the National Science Foundation (Grant CHE 1955552) is gratefully acknowledged.

REFERENCES

(1) Kramers, H. A. Brownian Motion in a Field of Force and the Diffusion Model of Chemical Reactions. *Physica* **1940**, *7*, 284−304.

(2) Zwanzig, R. *Nonequilibrium Statistical Mechanics.*; Oxford University Press: 2001.

(3) Chung, H. S.; Louis, J. M.; Eaton, W. A. Experimental determination of upper bound for transition path times in protein folding from single-molecule photon-by-photon trajectories. *Proc. Natl. Acad. Sci. U. S. A.* **2009**, *106* (29), 11837−44.

(4) Chung, H. S.; Louis, J. M.; Eaton, W. A. Single-molecule fluorescence experiments determine protein folding transition path times. *Science* **2012**, *335*, 981−984.

(5) Yu, H.; Gupta, A. N.; Liu, X.; Neupane, K.; Brigley, A. M.; Sosova, I.; Woodside, M. T. Energy landscape analysis of native folding of the prion protein yields the diffusion constant, transition path time, and rates. *Proc. Natl. Acad. Sci. U. S. A.* **2012**, *109* (36), 14452−7.

(6) Neupane, K.; Foster, D. A.; Dee, D. R.; Yu, H.; Wang, F.; Woodside, M. T. Direct observation of transition paths during the folding of proteins and nucleic acids. *Science* **2016**, *352* (6282), 239−42.

(7) Peters, B. *Reaction Theory and Rare Events*; Elsevier: 2017; p 634.
(8) Berezhkovskii, A. M.; Makarov, D. E. Communication: Transition-path velocity as an experimental measure of barrier crossing dynamics. *J. Chem. Phys.* **2018**, *148* (20), 201102.
(9) Hummer, G.; Szabo, A. Free energy profiles from single-molecule pulling experiments. *Proc. Natl. Acad. Sci. U. S. A.* **2010**, *107*, 21442−21446.
(10) Woodside, M. T.; Block, S. M. Reconstructing folding energy landscapes by single-molecule force spectroscopy. *Annu. Rev. Biophys.* **2014**, *43*, 19−39.
(11) Kolomeisky, A. B. *Motor Proteins and Molecular Motors*. CRC Press: 2015.
(12) Wang, H. Several Issues in Modeling Molecular Motors. *J. Comput. Theor. Nanosci.* **2008**, *5* (12), 2311−2345.
(13) Zhang, Q.; Brujic, J.; Vanden-Eijnden, E. Reconstructing Free Energy Profiles from Nonequilibrium Relaxation Trajectories. *J. Stat. Phys.* **2011**, *144* (2), 344−366.
(14) Lopez-Alamilla, N. J.; Jack, M. W.; Challis, K. J. Analysing single-molecule trajectories to reconstruct free-energy landscapes of cyclic motor proteins. *J. Theor. Biol.* **2019**, *462*, 321−328.
(15) Berkovich, R.; Fernandez, V. I.; Stirnemann, G.; Valle-Orero, J.; Fernandez, J. M. Segmentation and the Entropic Elasticity of Modular Proteins. *J. Phys. Chem. Lett.* **2018**, *9* (16), 4707−4713.
(16) Elber, R.; Makarov, D. E.; Orland, H. *Molecular Kinetics in Condense Phases: Theory, Simulation, and Analysis*; Wiley and Sons: 2020.
(17) Manuel, A. P.; Lambert, J.; Woodside, M. T. Reconstructing folding energy landscapes from splitting probability analysis of single-molecule trajectories. *Proc. Natl. Acad. Sci. U. S. A.* **2015**, *112* (23), 7183−8.
(18) Covino, R.; Woodside, M. T.; Hummer, G.; Szabo, A.; Cossio, P. Molecular free energy profiles from force spectroscopy experiments by inversion of observed committors. *J. Chem. Phys.* **2019**, *151* (15), 154115.
(19) Berezhkovskii, A. M.; Makarov, D. E. From Nonequilibrium Single-Molecule Trajectories to Underlying Dynamics. *J. Phys. Chem. Lett.* **2020**, *11* (5), 1682−1688.
(20) de Oliveira, R. J. Stochastic diffusion framework determines the free-energy landscape and rate from single-molecule trajectory. *J. Chem. Phys.* **2018**, *149* (23), 234107.
(21) Freitas, F. C.; Lima, A. N.; Contessoto, V. G.; Whitford, P. C.; Oliveira, R. J. Drift-diffusion (DrDiff) framework determines kinetics and thermodynamics of two-state folding trajectory and tunes diffusion models. *J. Chem. Phys.* **2019**, *151* (11), 114106.
(22) Avdoshenko, S. M.; Das, A.; Satija, R.; Papoian, G. A.; Makarov, D. E. Theoretical and computational validation of the Kuhn barrier friction mechanism in unfolded proteins. *Sci. Rep.* **2017**, *7* (1), 269.
(23) van Kampen, N. G. Remarks on Non-Markov Processes. *Brazilian Journal of Physics* **1998**, *28* (2), 90−96.
(24) Pyo, A. G. T.; Woodside, M. T. Memory effects in single-molecule force spectroscopy measurements of biomolecular folding. *Phys. Chem. Chem. Phys.* **2019**, *21* (44), 24527−24534.
(25) Nam, G. M.; Makarov, D. E. Extracting intrinsic dynamic parameters of biomolecular folding from single-molecule force spectroscopy experiments. *Protein Sci.* **2016**, *25*, 123−134.
(26) Makarov, D. E. Communication: Does force spectroscopy of biomolecules probe their intrinsic dynamic properties? *J. Chem. Phys.* **2014**, *141* (24), 241103.
(27) Neupane, K.; Woodside, M. T. Quantifying Instrumental Artifacts in Folding Kinetics Measured by Single-Molecule Force Spectroscopy. *Biophys. J.* **2016**, *111* (2), 283−6.
(28) Medina, E.; Satija, R.; Makarov, D. E. Transition Path Times in Non-Markovian Activated Rate Processes. *J. Phys. Chem. B* **2018**, *122* (49), 11400−11413.
(29) Berezhkovskii, A. M.; Makarov, D. E. Single-Molecule Test for Markovianity of the Dynamics along a Reaction Coordinate. *J. Phys. Chem. Lett.* **2018**, *9* (9), 2190−2195.
(30) Neupane, K.; Manuel, A. P.; Lambert, J.; Woodside, M. T. Transition-path probability as a test of reaction-coordinate quality reveals DNA hairpin folding is a one-dimensional diffusive process. *J. Phys. Chem. Lett.* **2015**, *6*, 1005−1010.
(31) Ozmaian, M.; Makarov, D. E. Transition path dynamics in the binding of intrinsically disordered proteins: A simulation study. *J. Chem. Phys.* **2019**, *151* (23), 235101.
(32) Satija, R.; Berezhkovskii, A. M.; Makarov, D. E. Broad distributions of transition-path times are fingerprints of multi-dimensionality of the underlying free energy landscapes. *Proc. Natl. Acad. Sci. U. S. A.* **2020**, *117*, 27116.
(33) Metzler, R.; Jeon, J. H.; Cherstvy, A. G.; Barkai, E. Anomalous diffusion models and their properties: non-stationarity, non-ergodicity, and ageing at the centenary of single particle tracking. *Phys. Chem. Chem. Phys.* **2014**, *16* (44), 24128−64.
(34) Daldrop, J. O.; Kappler, J.; Brunig, F. N.; Netz, R. R. Butane dihedral angle dynamics in water is dominated by internal friction. *Proc. Natl. Acad. Sci. U. S. A.* **2018**, *115* (20), 5169−5174.
(35) Daldrop, J. O.; Kowalik, B. G.; Netz, R. R. External potential modifies friction of molecular solutes in water. *Phys. Rev. X* **2017**, *7*, 041065.
(36) Satija, R.; Makarov, D. E. Generalized Langevin Equation as a Model for Barrier Crossing Dynamics in Biomolecular Folding. *J. Phys. Chem. B* **2019**, *123* (4), 802−810.
(37) Min, W.; Luo, G.; Cherayil, B. J.; Kou, S. C.; Xie, X. S. Observation of a power-law memory kernel for fluctuations within a single protein molecule. *Phys. Rev. Lett.* **2005**, *94* (19), 198302.
(38) Zijlstra, N.; Nettels, D.; Satija, R.; Makarov, D. E.; Schuler, B. Transition Path Dynamics of a Dielectric Particle in a Bistable Optical Trap. *Phys. Rev. Lett.* **2020**, *125*, 146001.
(39) Satija, R.; Das, A.; Muhle, S.; Enderlein, J.; Makarov, D. E. Kinetics of Loop Closure in Disordered Proteins: Theory vs Simulations vs Experiments. *J. Phys. Chem. B* **2020**, *124* (17), 3482−3493.
(40) Satija, R.; Das, A.; Makarov, D. E. Transition path times reveal memory effects and anomalous diffusion in the dynamics of protein folding. *J. Chem. Phys.* **2017**, *147* (15), 152707.
(41) Mehlich, A.; Fang, J.; Pelz, B.; Li, H.; Stigler, J. Slow Transition Path Times Reveal a Complex Folding Barrier in a Designed Protein. *Front. Chem.* **2020**, *8*, 587824.
(42) Li, H.; Xu, Y.; Li, Y.; Metzler, R. Transition path dynamics across rough inverted parabolic potential barrier. *Eur. Phys. J. Plus* **2020**, *135* (9), 731.
(43) Kim, J. Y.; Chung, H. S. Disordered proteins follow diverse transition paths as they fold and bind to a partner. *Science* **2020**, *368* (6496), 1253−1257.
(44) Hoffer, N. Q.; Neupane, K.; Pyo, A. G. T.; Woodside, M. T. Measuring the average shape of transition paths during the folding of a single biological molecule. *Proc. Natl. Acad. Sci. U. S. A.* **2019**, *116* (17), 8125−8130.
(45) Jacobs, W. M.; Shakhnovich, E. I. Accurate Protein-Folding Transition-Path Statistics from a Simple Free-Energy Landscape. *J. Phys. Chem. B* **2018**, *122*, 11126−11136.
(46) Kim, W. K.; Netz, R. R. The mean shape of transition and first-passage paths. *J. Chem. Phys.* **2015**, *143*, 224108.
(47) Makarov, D. E. Shapes of dominant transition paths from single-molecule force spectroscopy. *J. Chem. Phys.* **2015**, *143*, 194103.
(48) Cossio, P.; Hummer, G.; Szabo, A. Transition paths in single-molecule force spectroscopy. *J. Chem. Phys.* **2018**, *148*, 123309.
(49) Neupane, K.; Hoffer, N. Q.; Woodside, M. T. Measuring the Local Velocity along Transition Paths during the Folding of Single Biological Molecules. *Phys. Rev. Lett.* **2018**, *121*, 018102.
(50) Sega, M.; Faccioli, P.; Pederiva, F.; Garberoglio, G.; Orland, H. Quantitative protein dynamics from dominant folding pathways. *Phys. Rev. Lett.* **2007**, *99* (11), 118102.
(51) Carlon, E.; Orland, H.; Sakaue, T.; Vanderzande, C. Effect of Memory and Active Forces on Transition Path Time Distributions. *J. Phys. Chem. B* **2018**, *122* (49), 11186−11194.
(52) Gladrow, J.; Ribezzi-Crivellari, M.; Ritort, F.; Keyser, U. F. Experimental evidence of symmetry breaking of transition-path times. *Nat. Commun.* **2019**, *10* (1), 55.

https://dx.doi.org/10.1021/acs.jpcb.0c10978
J. Phys. Chem. B 2021, 125, 2467−2476

(53) Berezhkovskii, A. M.; Makarov, D. E. On the forward/backward symmetry of transition path time distributions in nonequilibrium systems. *J. Chem. Phys.* **2019**, *151*, 065102.
(54) Berezhkovskii, A. M.; Hummer, G.; Bezrukov, S. M. Identity of distributions of direct uphill and downhill translocation times for particles traversing membrane channels. *Phys. Rev. Lett.* **2006**, *97* (2), 020601.
(55) Chaudhury, S.; Makarov, D. E. A harmonic transition state approximation for the duration of reactive evennts in complex molecular rearrangements. *J. Chem. Phys.* **2010**, *133*, 034118.
(56) Makarov, D. E. *Single Molecule Science: Physical Principles and Models*; CRC Press, Taylor & Francis Group: Boca Raton, FL, 2015; p 214.
(57) Astumian, R. D. Microscopic reversibility as the organizing principle of molecular machines. *Nat. Nanotechnol.* **2012**, *7* (11), 684−8.
(58) Chung, H. S.; Eaton, W. A. Protein folding transition path times from single molecule FRET. *Curr. Opin. Struct. Biol.* **2018**, *48*, 30−39.
(59) Hoffer, N. Q.; Woodside, M. T. Probing microscopic conformational dynamics in folding reactions by measuring transition paths. *Curr. Opin. Chem. Biol.* **2019**, *53*, 68−74.
(60) Sturzenegger, F.; Zosel, F.; Holmstrom, E. D.; Buholzer, K. J.; Makarov, D. E.; Nettels, D.; Schuler, B. Transition path times of coupled folding and binding reveal the formation of an encounter complex. *Nat. Commun.* **2018**, *9* (1), 4708.
(61) Kim, J.-Y.; Meng, F.; Yoo, J.; Chung, H. S. Diffusion-limited association of disordered protein by non-native electrostatic interactions. *Nat. Commun.* **2018**, *9* (1), 4707.
(62) Neupane, K.; Manuel, A. P.; Woodside, M. Protein folding trajectories can be described quantitatively by one-dimensional diffusion over measured energy landscapes. *Nat. Phys.* **2016**, *12*, 700−703.
(63) Cheng, R. R.; Makarov, D. E. Failure of one-dimensional Smoluchowski diffusion models to describe the duration of conformational rearrangements in floppy, diffusive molecular systems: a case study of polymer cyclization. *J. Chem. Phys.* **2011**, *134* (8), 085104.
(64) Zheng, W.; Best, R. B. Reduction of All-Atom Protein Folding Dynamics to One-Dimensional Diffusion. *J. Phys. Chem. B* **2015**, *119* (49), 15247−55.
(65) Pollak, E. Transition path time distribution and the transition path free energy barrier. *Phys. Chem. Chem. Phys.* **2016**, *18* (41), 28872−28882.
(66) Herrera-Delgado, E.; Briscoe, J.; Sollich, P. Tractable nonlinear memory functions as a tool to capture and explain dynamical behaviors. *Physical Review Research* **2020**, *2*, 043069.
(67) Lapolla, A.; Godec, A. Manifestations of Projection-Induced Memory: General Theory and the Tilted Single File. *Front. Phys.* **2019**, *7*, 182.
(68) Mori, T.; Saito, S. Molecular Mechanism Behind the Fast Folding/Unfolding Transitions of Villin Headpiece Subdomain: Hierarchy and Heterogeneity. *J. Phys. Chem. B* **2016**, *120* (45), 11683−11691.

https://dx.doi.org/10.1021/acs.jpcb.0c10978
J. Phys. Chem. B 2021, 125, 2467−2476